Transient Stability Assessment of Two-Area Power System with Robust Controller based CSC-STATCOM

Sandeep Gupta, Ramesh Kumar Tripathi

Department of Electrical Engineering
M.N.N.I.T. Allahabad, INDIA
E-mail: guptavilab@gmail.com, rktripathi@mnnit.ac.in

Abstract: A Current source converter (CSC) based static synchronous compensator (STATCOM) is a shunt flexible ac transmission system (FACTS) device, which has a vital role as a stability support for small and large transient instability in an interconnected power network. A robust pole-shifting based controller for CSC-STATCOM is proposed. In this paper, pole-shifting controller based CSC-STATCOM is designed for enhance the transient stability of two-area two-machine power system. First of all, modeling & pole-shifting controller design for CSC-STATCOM are described. After that, to show the impact of proposed scheme on the test system with different disturbances. Here, applicability of the proposed scheme is demonstrated through simulation in MATLAB and the simulation results show an improvement in the transient stability of power system with CSC-STATCOM. Also clearly show, the robustness and effectiveness of CSC-STATCOM are better rather than other shunt FACTS devices (SVC & VSC-STATCOM) in this paper.

Keywords: CSC, FACTS, Pole-shifting, Power system stability, STATCOM.

1. INTRODUCTION

The continuous development of electrical loads due to the modification of society structure result in today's transmission structure to be faced close to their stability restrictions. So the renovation of urban and rural power network is more and more necessary. Due to governmental, financial and green climate reasons, it is not always possible to construct new transmission lines to relieve the power system stability problem at the existing overloaded transmission lines. As a result, the utility industry is facing the challenge of efficient utilization of the existing AC transmission lines in power system networks. So transient stability, voltage regulation, damping oscillations etc are the most important operating issues that electrical engineers are facing during power-transfer at high levels.

In above power quality problems, transient stability is the one of the most important key factor during power-transfer at high levels. According to literature, transient stability of a power system is its ability to maintain synchronous operation of the machines when subjected to a large disturbance (Kundur, 1994). While generator excitation system can maintain excitation control but it is not adequate to sustain stability of power system for large faults or overloading occur near to generator terminals (Law, 1994). So many researchers worked on this problem for finding the solution since a long time. In between solutions, one of the powerful methods for enhance the transient stability is to use flexible AC transmission system (FACTS) devices (Hammad, 1986; Cong *et al.,* 2002; Hosseine *et al.*, 2002; Tan *et al.*, 2004; Haque *et al.*, 2004). Even though the prime objective of shunt FACTS devices (SVC, STATCOM) is to maintain bus voltage by absorbing (or injecting) reactive power, they are also competent of improving the system transient stability by diminishing (or increasing) the capability of power transfer when the machine angle decreases (increases), which is accomplished by operating the shunt FACTS devices in inductive (capacitive) mode (Gyugyi, 1988).

In many cited research papers (Hammad, 1986; Tan *et al.*, 2004; Jing *et al.*, 1995; Tsai *et al.*, 2005, Rangasamy *et al.*, 2014), the different types of these devices and with different control techniques are used to improving transient stability. In between these devices, the STATCOM is valuable for enhancement stability and frequency stabilization due to the more rapidly output response, lower harmonics, superior control stability and small size etc. (Haque, 2004; Tan, 1999). By their inverter configuration, basic Type of STATCOM topology can be realized by either a current-source converter (CSC) or a voltage-source converter (VSC) (Hingorani *et al.*, 1999; Gyugyi *et al.*, 2000; Schauder *et al.*, 1997; Han *et al.*, 2000; Sandeep *et al.*, 2010). But Recent research confirms several merits of CSC based STATCOM over VSC based STATCOM (Shen *et al.*, 2002; Kazearni *et al.*, 2002; Ye *et al.*, 2005). These advantages are high converter reliability, quick starting, inherent short-circuit protection, the output current of converter is directly controlled, in low switching frequency this reduces the filtering requirements compared with the case of a VSC. Therefore CSC based STATCOM is very useful in power systems rather than VSC based STATCOM in many cases.

Presently the most used techniques for controller design of FACTS devices are the Proportional Integration (PI), PID controller (Ni *et al.*, 1998), pole placement and linear quadratic regulator (LQR) (Ali *et al.*, 2007; Pedro *et al.*,

2013). But LQR and pole placement algorithms give the quick response in comparison to PI & PID algorithm and LQR controller Gain (K) can be calculated by solving the riccati equation and K is also dependent on the two cost function (Q, R) (Rao *et al.*, 2000). Riccati equation solvers have some limitations, which are related to the input arguments. But pole shifting method does not face this type of any problem. So pole shifting method gives better and robust performance in comparison to other methods.

The main contribution of this paper is the application of the pole-shifting controller based CSC-STATCOM for transient stability improvement of power system by injecting (or absorbing) reactive power. In this paper, the proposed pole-shifting controller based CSC-STATCOM is used in Two area power system with dynamic loads under a grievous disturbance conditions (three phase fault or heavy loading) to enhancement of transient stability studies and observe impact of the CSC-STATCOM on electromechanical oscillations and transmission capacity. Furthermore, the obtained outcomes from the proposed algorithm based CSC-STATCOM are compared to the obtained outcomes from the other shunt FACTS devices (SVC & VSC based STATCOM) which are used in previous works (Sidhartha *et al.*, 2006; Sybille *et al.*, 2002). This paper results are demonstrated through MATLAB simulation.

The rest of paper is prepared as follows. Section-2 discusses about the circuit modeling & pole-shifting controller designing of CSC based STATCOM. A two-area tow-machine power system is described with a CSC-STATCOM device in Section-3. Simulation results of the test system with different shunt FACTS devices (SVC, VSC-STATCOM, and CSC-STATCOM) for severe contingency are shown in Section-4, to improve transient stability of system. Finally, Section-5 concludes this paper.

2. MATHEMATICAL MODELING OF POLE-SHIFTING CONTROLLER BASED CSC-STATCOM

2.1 CSC based STATCOM model

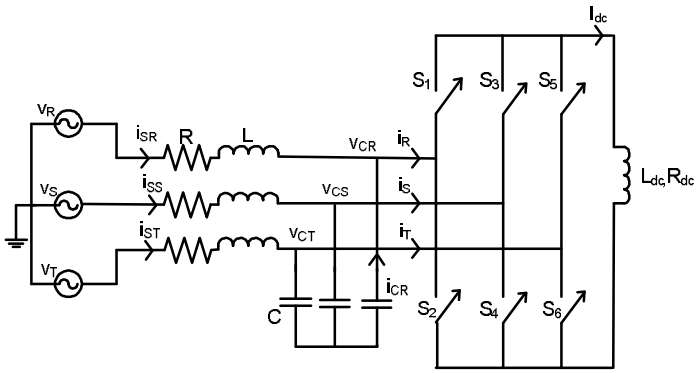

Fig. 1. The representation of CSC based STATCOM.

Where

i_R, i_S, i_T	line current;
v_{CR}, v_{CS}, v_{CT}	voltages across the filter capacitors;
v_R, v_S, v_T	line voltages;
I_{dc}	dc-side current;
R_{dC}	converter switching and conduction losses;
L_{dc}	smoothing inductor;
L	inductance of the line reactor;
R	resistance of the line reactor,

To verify the response of the STATCOM on dynamic performance, the mathematical modeling and control strategy of a CSC based STATCOM are needed to be presented. So in the designing of controller for CSC based STATCOM, the state space equations from the CSC-STATCOM circuit must be introduced. For minimize the complexity of mathematical calculation, the theory of dq transformation of currents has been applied in this circuit, which makes the d and q components as independent parameters. Fig. 1 shows the circuit diagram of a typical CSC based STATCOM.

The mathematical model of the STATCOM has been derived in the literature (Ye *et al.*, 2005). Therefore, only a brief detail of the test-system is given here for the readers' convenience. Based on the equivalent circuit of CSC-STATCOM shown in fig.1, the differential equations can be achieved for the system, which are derived in the abc frame and then transformed into the synchronous dq frame using dq transformation method (Schauder *et al.*, 1993).

$$\frac{d}{dt}I_{dc} = -\frac{R_{dc}}{L_{dc}}I_{dc} - \frac{3}{2L_{dc}}M_d V_d - \frac{3}{2L_{dc}}M_q V_q \tag{1}$$

$$\frac{d}{dt}I_d = -\frac{R}{L}I_d + \omega I_q - \frac{1}{L}\frac{E_d}{n} + \frac{1}{L}V_d \tag{2}$$

$$\frac{d}{dt}I_q = -\omega I_d - \frac{R}{L}I_q + \frac{1}{L}V_q \tag{3}$$

$$\frac{d}{dt}V_d = -\frac{1}{C}I_d + \omega V_q + \frac{1}{C}M_d I_{dc} \tag{4}$$

$$\frac{d}{dt}V_q = -\frac{1}{C}I_q - \omega V_d + \frac{1}{C}M_q I_{dc} \tag{5}$$

In above differential equations M_d and M_q are the two input variables. Two output variables are I_{dc} and I_q. Here, ω is the rotation frequency of the system and this is equal to the nominal frequency of the system voltage. These above equations (1 to 5) are shown that controller for CSC based STATCOM has nonlinearity characteristic. This nonlinear property can be removed by accurately modeling of CSC based STATCOM. From above equations (1)-(5), nonlinear property in CSC-STATCOM model is due to the part of I_{dc}. This nonlinear property is removed with the help of active power balance equation. So the power loss in the switches and resistance R are ignored in this system. After using power balance equation and mathematical calculation, nonlinear characteristic is removed from (5). Finally obtained the equation below:

$$\frac{d}{dt}\left(I_{dc}^2\right) = -\frac{2R_{dc}}{L_{dc}}\left(I_{dc}^2\right) - \frac{3E_d}{L_{dc}n}I_d \tag{6}$$

In above (6) state variable (I_{dc}) is replaced by the state variable (I^2_{dc}), to make the dynamic equation linear. Finally the resulting better dynamic and robust model of the SATACOM in matrix form can be derived as:

$$\frac{d}{dt}\begin{bmatrix} (i_{dc})^2 \\ i_d \\ i_q \\ v_{cd} \\ v_{cq} \end{bmatrix} = \begin{bmatrix} -\frac{2R_{dc}}{L_{dc}} & \frac{3E_d}{L_{dc}n} & 0 & 0 & 0 \\ 0 & -\frac{R}{L} & \omega_o & \frac{1}{L} & 0 \\ 0 & -\omega_o & -\frac{R}{L} & 0 & \frac{1}{L} \\ 0 & -\frac{1}{C} & 0 & 0 & \omega_o \\ 0 & 0 & -\frac{1}{C} & -\omega_o & 0 \end{bmatrix} * \begin{bmatrix} (i_{dc})^2 \\ i_d \\ i_q \\ v_{cd} \\ v_{cq} \end{bmatrix} + \begin{bmatrix} 0 & 0 \\ 0 & 0 \\ 0 & 0 \\ \frac{1}{C} & 0 \\ 0 & \frac{1}{C} \end{bmatrix} * \begin{bmatrix} I_{id} \\ I_{iq} \end{bmatrix} + \begin{bmatrix} 0 \\ -\frac{1}{L} \\ 0 \\ 0 \\ 0 \end{bmatrix} * E_d \quad (7)$$

Above modeling of CSC based STATCOM is written in the form of modern control methods i.e. State-space representation. For state-space modeling of the system, section 2.2 is considered.

2.2 Pole-shifting Controller Design:

Pole shift technique is one of the basic control methods which employed in feedback control system theory. Theoretically Pole shift technique is to set the preferred pole position and to move the pole position of the system to that preferred pole position, to get the desired system outcomes. Here poles of system are shifted because the position of the poles related directly to the eigenvalues of the system, which control the dynamic characteristics of the system outcomes (Vasile *et al.*, 2009). But for this method, the system must be controllable.

In the dynamic modeling of systems, State-space equations involve three types of variables: state variables(x), input(u) and output variables (y) with disturbance (e). So comparing (7) with the standard state-space representation i.e.

$$\dot{x} = Ax + Bu + Fe \quad (8)$$

$$y = Cx \quad (9)$$

The system matrices get as:

$$x = \begin{bmatrix} I^2_{dc} & I_d & I_q & V_d & V_q \end{bmatrix}^T$$

$$u = \begin{bmatrix} I_{id} & I_{iq} \end{bmatrix}^T \qquad e = E_d \qquad y = \begin{bmatrix} I^2_{dc} & I_q \end{bmatrix}^T$$

$$A = \begin{bmatrix} -\frac{2R_{dc}}{L_{dc}} & -\frac{3E_d}{L_{dc}} & 0 & 0 & 0 \\ 0 & -\frac{R}{L} & \omega & \frac{1}{L} & 0 \\ 0 & -\omega & -\frac{R}{L} & 0 & \frac{1}{L} \\ 0 & -\frac{1}{c} & 0 & 0 & \omega \\ 0 & 0 & -\frac{1}{c} & -\omega & 0 \end{bmatrix}$$

$$B = \begin{bmatrix} 0 & 0 \\ 0 & 0 \\ 0 & 0 \\ \frac{1}{c} & 0 \\ 0 & \frac{1}{c} \end{bmatrix} \quad ; \quad C = \begin{bmatrix} 1 & 0 \\ 0 & 0 \\ 0 & 1 \\ 0 & 0 \\ 0 & 0 \end{bmatrix}^T \quad ; \quad F = \begin{bmatrix} 0 \\ -\frac{1}{L} \\ 0 \\ 0 \\ 0 \end{bmatrix}$$

In above equations (8, 9) five system states, two control inputs and two control outputs are presented. Where x is the state vector, u is the input vector, A is the basis matrix, B is the input matrix, e is disturbance input.

If controller is set as:

$$u = -Kx + Ty_{ref} + Me \quad (10)$$

Then the state equation of closed loop can be written as

$$\dot{x} = (A - BK)x + Ty_{ref} + BMe + Fe \quad (11)$$

has the desired specifications. Here K is the state-feedback gain matrix. The gain matrix K is designed in such a way that equation (12) is satisfied with the desired poles.

$$\left| sI - (A - BK) \right| = (s - P_1)(s - P_2).....(s - P_n) \quad (12)$$

Where P_1, P_2, …..P_n are the desired pole locations. Equation (12) is the desired characteristic polynomial equation. The values of P_1, P_2, …..P_n are selected such as system becomes stable and all closed-loop eigenvalues are located in the left half of the complex-plane. The final configuration of the proposed pole-shifting controller based CSC-STATCOM is shown in Fig. 2.

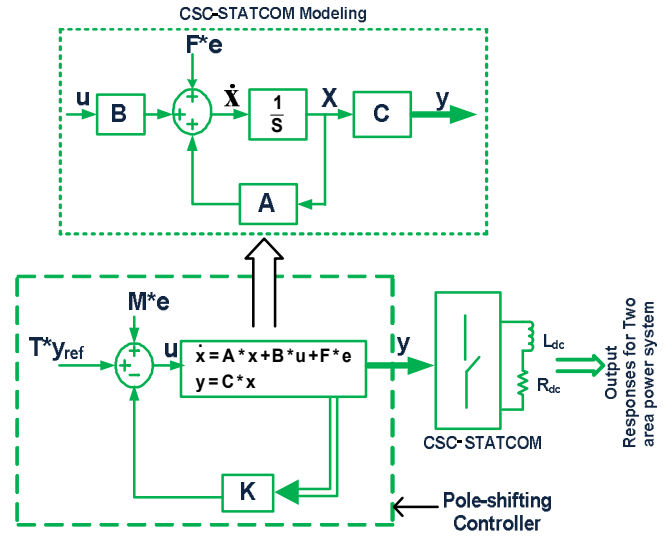

Fig. 2. Control Structure of pole-shifting controller based CSC-STATCOM.

3. TWO AREA POWER SYSTEM WITH CSC-STATCOM FACTS DEVICE

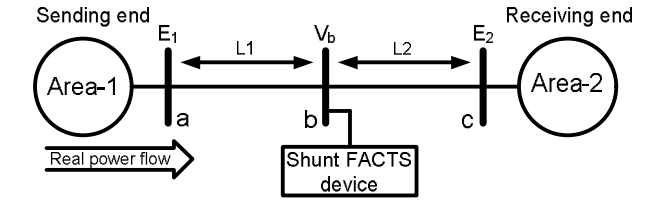

(a)

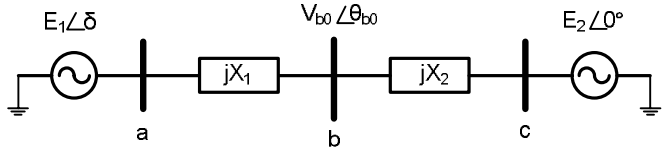

(b)

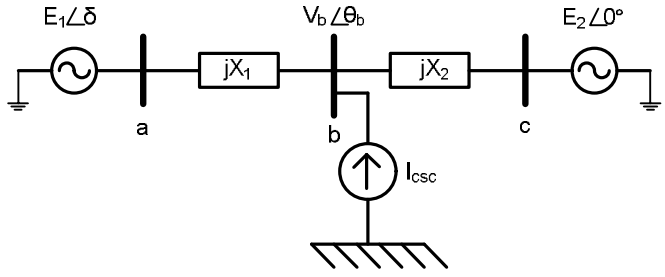

(c)

Fig. 3. A two-area two-machine power system with CSC-STATCOM; (a) A single line diagram; (b) Simplified model of the test system without CSC-STATCOM; (c) Simplified model of the test system with a CSC-STATCOM as a current injection device.

Firstly consider a two-area two-machine power system with a CSC-STATCOM at bus b is connected through a long transmission system. Fig. 3 shows this representation. Fig. 3(b) represents the equivalent circuit of test system without CSC-STATCOM. Here path of active power flow is from area 1 to area 2. Fig. 3(c) represents the equivalent circuit of the test system with a CSC-STATCOM, where CSC-STATCOM is used as shunt current source device.

The dynamic model of the machine, with a CSC-STATCOM, can be written in the differential algebraic equation form as follows:

$$\dot{\delta} = \omega \tag{13}$$

$$\dot{\omega} = \frac{1}{M}\left[P_m - P_{eo} - P_e^{csc}\right] \tag{14}$$

Here ω is the rotor speed, δ is the rotor angle, P_m is the mechanical input power of generator, the output electrical power without CSC-STATCOM is represents by P_{eo} and M is the moment of inertia of the rotor. Equation (14) is also called as swing equation. The additional factor of the output electrical power of generator from a CSC-STATCOM is P_e^{csc} in the swing equation. From Fig. 3(b), output of generator (P_{eo}) is

$$P_{eo} = \frac{E_1 V_{bo}}{X_1}\sin(\delta - \theta_{bo}) = \frac{E_1 E_2}{X_1 + X_2}\sin(\delta) \tag{15}$$

Where V_{bo} and θ_{bo} are voltage magnitude and angle at bus b in absentia of CSC-STATCOM, which are computed as follows:

$$\theta_{bo} = \tan^{-1}\left[\frac{X_2 E_1 \sin\delta}{X_2 E_1 \cos\delta + X_1 E_2}\right] \tag{16}$$

$$V_{bo} = \left(\frac{X_2 E_1 \cos(\delta - \theta_{bo}) + X_1 E_2 \cos\theta_{bo}}{X_1 + X_2}\right) \tag{17}$$

After this for calculation of P_e^{csc}, the Fig. 3(c) is considered and assumed that CSC-STATCOM is worked in capacitive mode. Then the injected current from CSC-STATCOM to test system can be written as:

$$I_{csc} = I_{csc}\angle(\theta_{bo} - 90^o) \tag{18}$$

In Fig. 3(c), the magnitude (V_b) and angle (θ_b) of voltage at bus b can be computed as (Kumkratug *et al.*, 2003):

$$\theta_b = \tan^{-1}\left[\frac{X_2 E_1 \sin\delta}{X_2 E_1 \cos\delta + X_1 E_2}\right] \tag{19}$$

$$V_b = \left(\frac{X_2 E_1 \cos(\delta - \theta_{bo}) + X_1 E_2 \cos\theta_{bo}}{X_1 + X_2}\right) + \left(\frac{X_1 X_2}{X_1 + X_2} I_{csc}\right) \tag{20}$$

From (20), the voltage magnitude of bus b (V_b) depends on the STATCOM current I_{csc}. In Fig. 3(c), the electrical output

power P_e^{csc} of machine due to a CSC-STATCOM, can be expressed as

$$P_e^{csc} = \frac{E_1 V_b}{X_1}\sin(\delta - \theta_b) \quad (21)$$

Finally, using (20) & (21) the total electrical output (P_e) of machine with CSC-STATCOM can be written as

$$P_e = P_{eo} + P_e^{csc} \Longrightarrow P_{eo} + \frac{X_1 X_2 E_1}{(X_1 + X_2)X_1} I_{csc}\sin(\delta - \theta_b) \quad (22)$$

All above equations are represented for capacitive mode of CSC-STATCOM. But I_{csc} is replaced by $-I_{csc}$ in (18), (20) & (22) for inductive mode of operation. With the help of (14), the power-angle curve of the test system for stability analysis can be drawn as shown in Fig. 4.

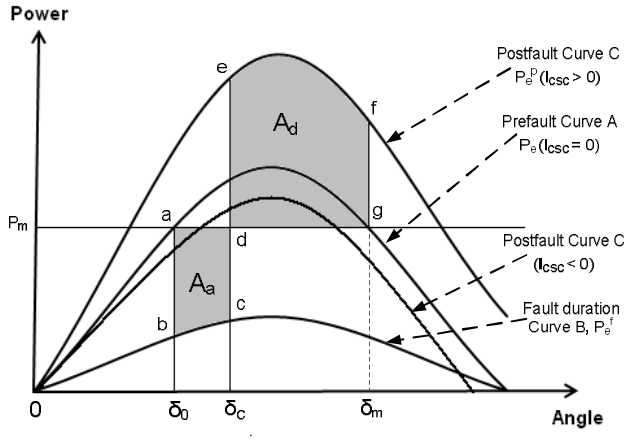

Fig. 4. Power-Angle characteristic of the test system with a CSC-STATCOM.

The power-angle (P-δ) curve of the test system without a CSC-STATCOM is representing by curve A (also called Prefault condition) in Fig. 4. Here mechanical input is P_m , electrical output is P_e and initial angle is δ_0. When a fault occurs, P_e suddenly decreases and the operation shifts from point a to point b at curve B and thus the machine starts accelerating from point b to point c, where accelerating power P_a [= $(P_m - P_e)$] >0. At fault clearing, P_e suddenly increases and the area a-b-c-d-a represents the accelerating area A_a as defined in (23). If the CSC-STATCOM operates in capacitive mode (at fault clearing), P_e increases to point e at curve C (also called postfault condition). In this time P_a is negative. Thus the machine starts decelerating but its angle continues increasing from point e to point f until reaches a maximum allowable value δ_m at point f, for system stability. The area e-f-g-d-e represents the decelerating area A_d as defined in (23). From previous literature (Kundur, 1994), equal area criterion for stability of system can be written as:

$$\int_{\delta_0}^{\delta_c}\left(P_m - P_e^f\right)d\delta = \int_{\delta_c}^{\delta_m}\left(P_e^p - P_m\right)d\delta \Longrightarrow A_a = A_d \quad (23)$$

This equation is generated from Fig. 4, where δ_c is critical clearing angle. P_e^p is electrical output for post-fault condition. P_e^f is electrical output during fault condition. From Fig. 4 clearly see, for capacitive mode of operation (I_{csc}>0), the P-δ curve is not only uplifted but also displacement toward right and that endues more decelerating area and hence higher stability limit. After that section 4 is considered for verify the impact of above written theory and analysis of the test-system stability.

4. SIMULATION RESULTS

4.1 Power system under study:

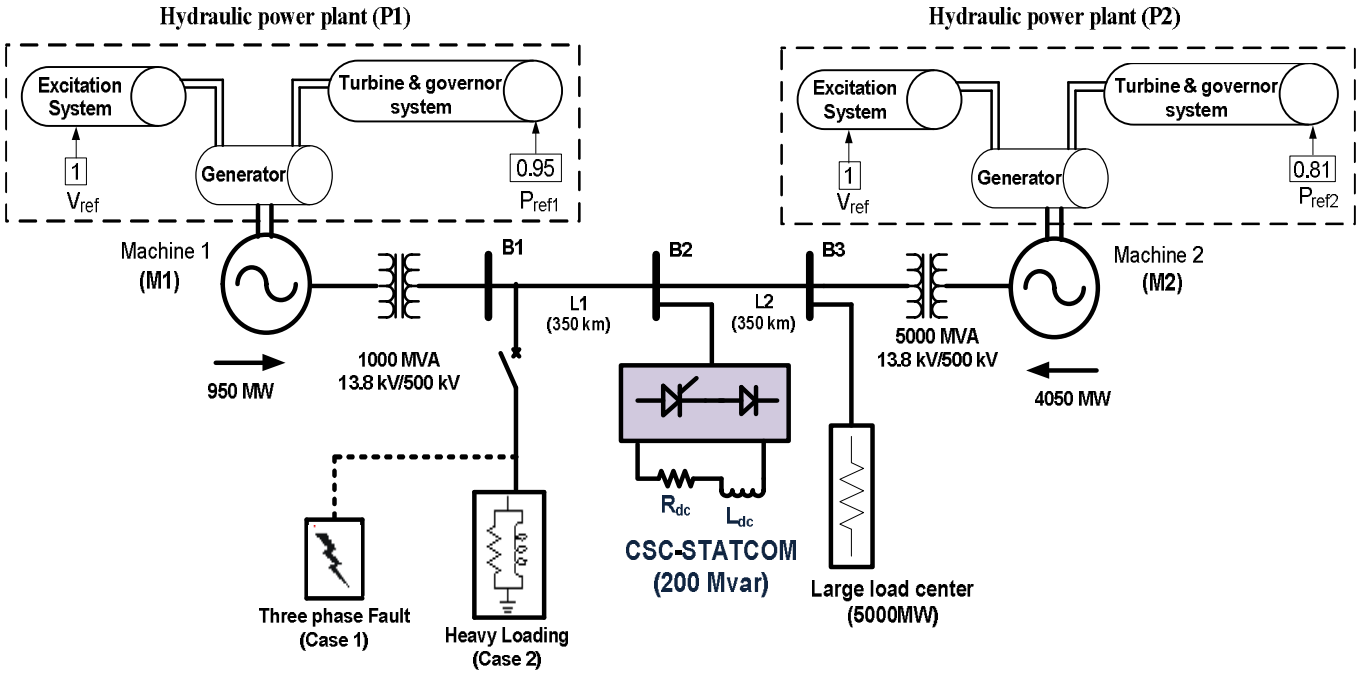

Fig. 5. The test model diagram with different shunt FATCS devices for transient stability study of two power plants (P1 & P2).

In this section, two area power system theory is consider for the test system study. For this type of test system, a 500-kV transmission system with two hydraulic power plants (P1 (machine 1) & P2 (machine 2)) connected through 700-km long transmission line is taken as shown in Fig. 5. Rating of first power generation plant (P1) is 13.8kv/1000MVA, which is used as PV generator bus type. Electrical output of second power plant (P2) is 5000MVA, which is used as swing bus for balancing the power. One 5000 MW large resistive load is connected near the plant P2 as shown in Fig. 5. To maintain the synchronism of plants (i.e. machine 1 & 2) and improved the transient stability of above test system after disturbances (faults or heavy loading), a 200 Mvar CSC-STATCOM is connected at the mid-point of transmission line. In order to previous work (Ooi *et al.*, 1997), shunt FACTS devices give maximum efficiency when connected at the mid-point of transmission line. Here the two hydraulic generating units are assembled with a turbine-governer set and excitation system. But hydraulic generating unit is not explained in this paper. This is explained in the reference (Kundur, 1994). Here one more point should be clear that any shunt FACTS device does not have a power oscillation damping (POD) unit in this paper. All the data required to this test system model are given in Appendix A.

Now a severe contingency will be apply on the test system and observe the impact of CSC based STATCOM for maintain the system stability through MATLAB/SIMULINK.

***Case 1**-Short-circuit fault:*

For this case, it is considered that a three-phase fault is occurred at near bus B1 at t=0.1 s and is cleared at 0.23 s. The impact of system with & without CSC based STATCOM to this disturbance are shown in Fig. 6 to Fig.11. Simulation is carried out for 8 s to observe the nature of transients. It is clear that the system without CSC-STATCOM is unstable upon the clearance of the fault from Fig. 6 & 7. But this system with CSC-STATCOM is restored and stable upon the clearance of the fault from Fig. 8 to Fig. 11. Synchronism in between machines M1 & M2 is also maintained in Fig. 9 & 10. Here the critical clearing time (CCT) of fault is also found out for the test system stability by trial and error method. CCT is defined as maximal fault duration for which the system remains transiently stable (Kundur, 1994). CCT of the fault for system with & without CSC-STATCOM are 286 ms and 225 ms respectively, as shown in Table-1. So it is clearly say that CCT of fault is also increased due to the impact of CSC-STATCOM.

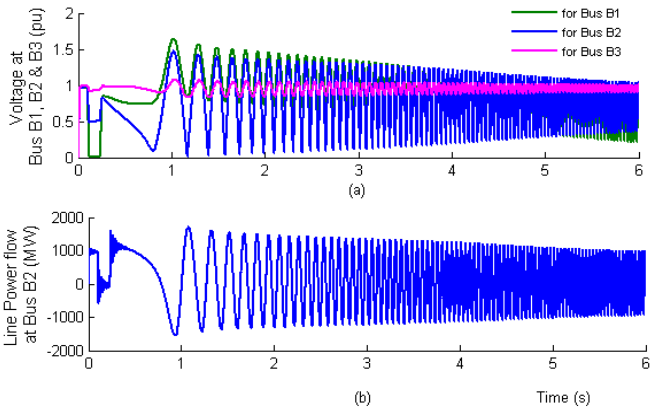

Fig. 6. Test system response without CSC-STATCOM for a three phase fault (Case-1). (a) Positive sequence voltages at different buses B1, B2 & B3 (b) Power flow at bus B2.

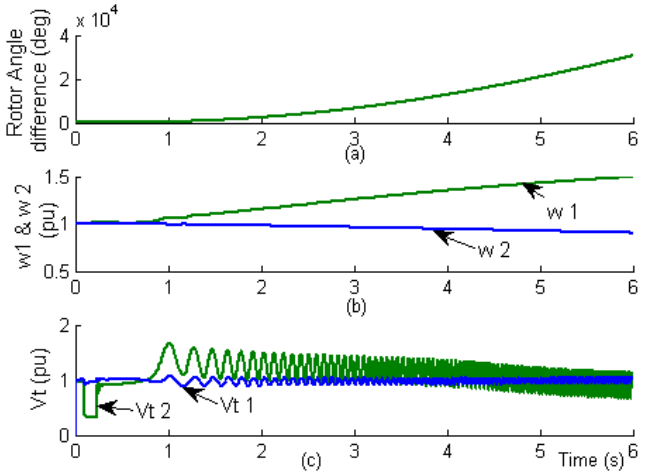

Fig. 7. System response without CSC-STATCOM for Case-1 (a) Difference between Rotor angles of machines M1 & M2 (b) w1 & w2 speeds of machine M1 & M2 respectively (c)terminal voltages Vt1 & Vt2 of generators M1 & M2 respectively.

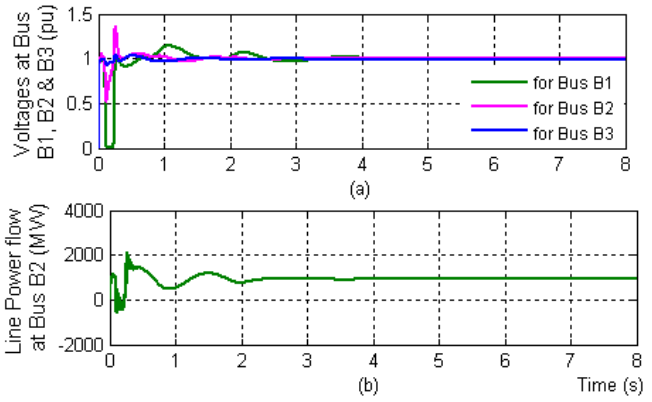

Fig. 8. Test-system response with CSC-STATCOM for a three phase fault (Case-1). (a) Positive sequence voltages at different buses B1, B2 & B3 (b) Power flow at bus B2.

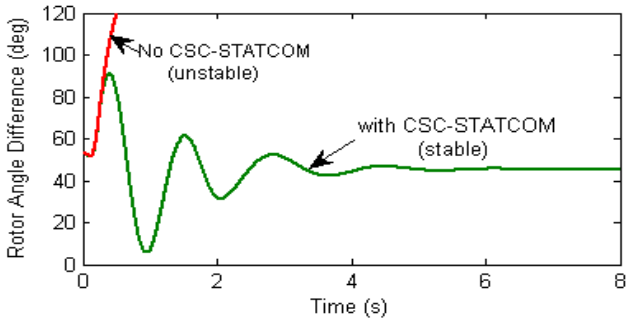

Fig. 9. Rotor angles difference of machines M1 & M2 for case-1.

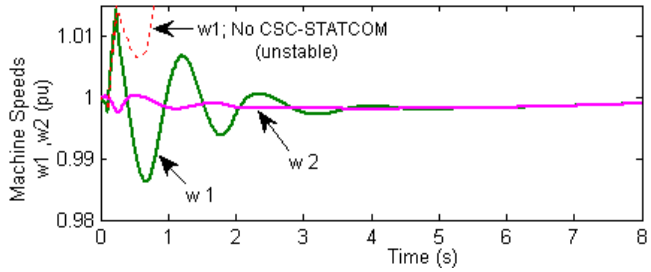

Fig. 10. Machine speeds w1 & w2 with CSC-STATCOM for case-1.

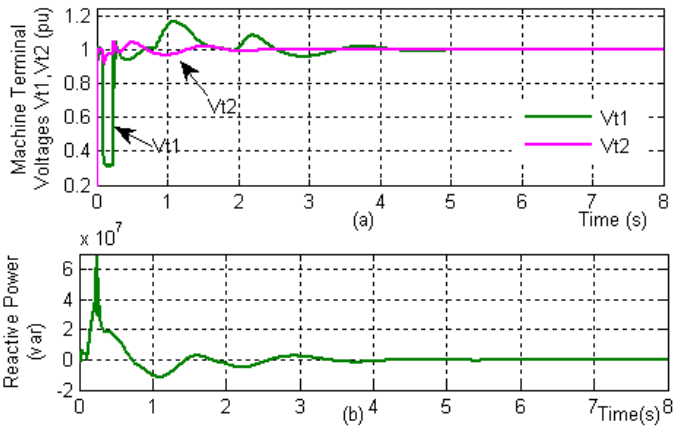

Fig. 11. For case-1 (a) terminal voltages Vt1 & Vt2 of generators M1 & M2 with CSC-STATCOM respectively (b) reactive power inject (or absorb) by CSC-STATCOM.

***Case 2**-Large loading:*

For heavy loading case, one large load centre (10000MW/5000Mvar) is connected at near bus B1 (i.e. at near plant P1) in Fig. (5). This large loading is occurred only at time period 0.1 s to 0.5 s. Due to this disturbance, simulation results of test system with and without CSC-STATCOM are shown in Fig. 12 to Fig. 16. Clearly, the system is unstable in the absence of CSC based STATCOM device due to this disturbance in Figs. 14 & 15 (in terms of machine rotor angle differences, machine speeds). But system with CSC-STATCOM is continuing stable condition in Fig. 13 to Fig. 15. Fig. 16 also shows that how much reactive power injected or absorbed by CSC-STATCOM to the test system for maintaining the system stability. Here CCT for the system with & without CSC-STATCOM are 585 ms & 442 ms respectively, which are provided in Table 1. Clearly, CCT for test system is better due to the impact of CSC-STATCOM. So performance of the pole-shifting controller based CSC-STATCOM is still satisfactory in this case.

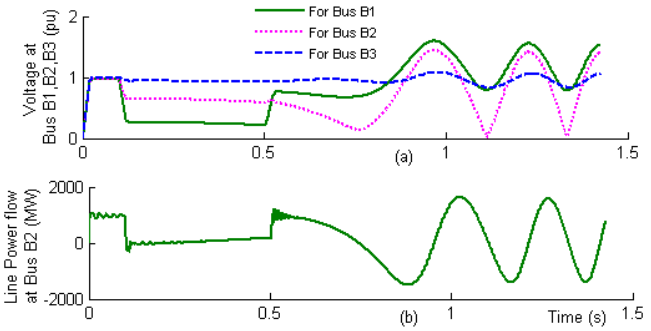

Fig. 12. The test system response without CSC-STATCOM for a heavy loading (Case-2). (a) Positive sequence voltages at different buses B1, B2 & B3 (b) Power flow at bus B2.

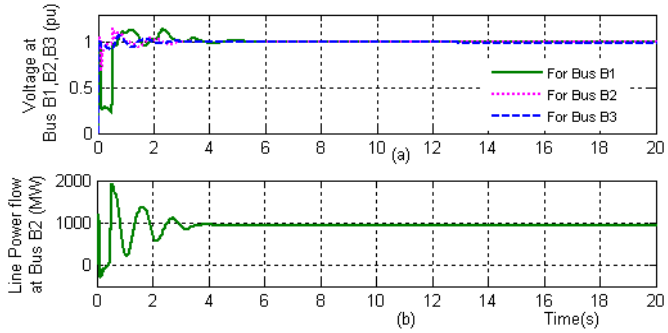

Fig. 13. The test system response with CSC-STATCOM for a heavy loading (Case-2). (a) Positive sequence voltages at different buses B1, B2 & B3 (b) Power flow at bus B2.

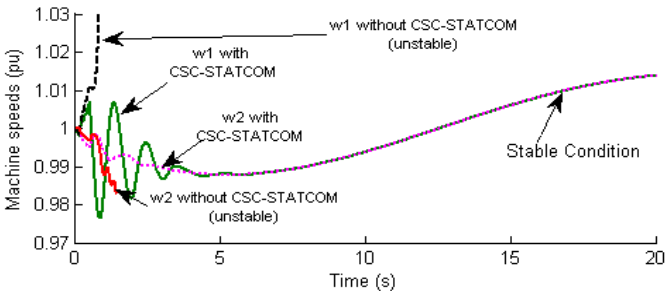

Fig. 14. Speeds w1 & w2 for machines M1 & M2 respectively for case-2.

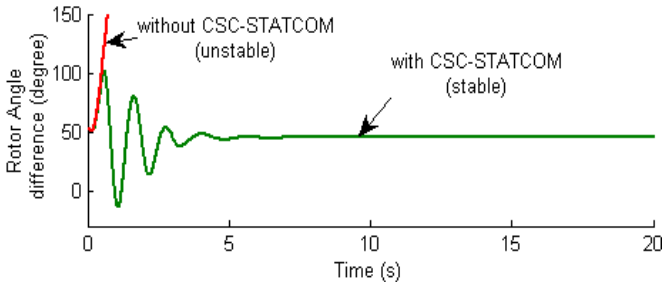

Fig. 15. Rotor angle difference of machines M1 & M2 for system with and without CSC-STATCOM in case-2.

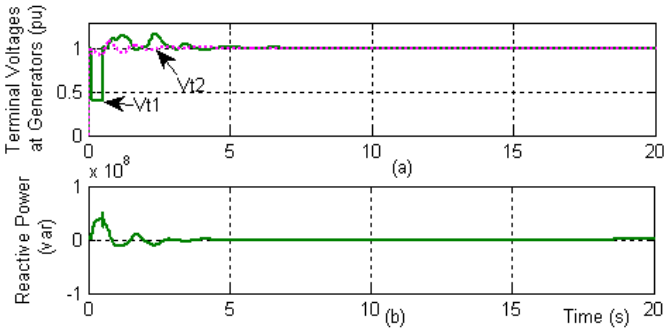

Fig. 16. For case-2 (a) terminal voltages Vt1 & Vt2 of generators M1 & M2 with CSC-STATCOM respectively (b) reactive power inject (or absorb) by CSC-STATCOM.

***Case 3**-A comparative study:*

In order to show the robustness performance of the proposed scheme for improving the transient stability of system, after this obtained outcomes from the proposed controller based CSC-STATCOM are compared to the obtained outcomes from the other shunt FACTS devices (SVC and VSC based STATCOM) which have been used in some most cited papers (Sidhartha *et al.*, 2006; Sybille *et al*, 2002). In this case, I have assumed that the test system is same for all shunt FACTS devices and rating of all shunt FACTS devices (200MVAR) is also same. After this, to check the impact of these shunt FACTS devices on the test system with three phase fault condition. The obtained simulation results with theses shunt FACTS devices are compared in Fig. 17. Here three phase fault duration is 0.1 s to 0.2 s. CCT for the system with different shunt FACTS devices are shown in Table-1. If three-phase fault duration is increased (at 0.1 s to 0.24 s). Then system with SVC is reached in unstable condition. This is shown in Fig. 18. Clearly, Waveforms show that CSC-STATCOM is more effective and robustness performance than that of other shunt FACTS devices (SVC & VSC-STATCOM) in terms of oscillation damping, settling time, CCT and transient stability of the test-system in Figs. 17 & 18.

Table 1. CCT of disturbances for the test system stability with different shunt FACTS devices.

S.No.	FACTS devices	Critical Clearing Time (CCT)
Case-1	Without CSC-STATCOM	100 ms – 221 ms
	With CSC-STATCOM	100 ms – 282 ms
Case-2	Without CSC-STATCOM	100 ms – 442 ms
	With CSC-STATCOM	100 ms – 579 ms
Case-3	With SVC	100 ms – 234 ms
	With VSC-STATCOM	100 ms – 239 ms
	With CSC-STATCOM	100 ms – 282 ms

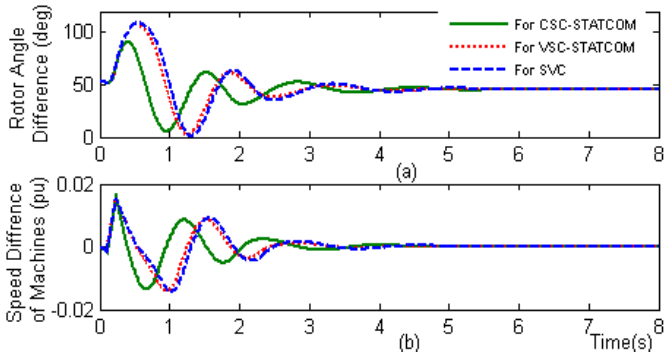

Fig. 17. System response with different shunt FACTS devices (CSC-STATCOM, VSC-STATCOM & SVC) for Case-3 (a) Difference between Rotor angles of machines M1 & M2 (b) speed difference of machines M1 & M2.

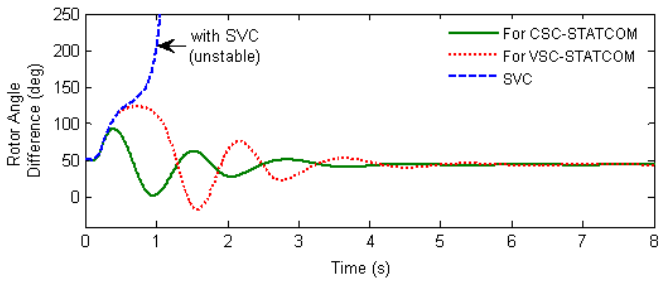

Fig. 18. Rotor angles Difference of machines M1 & M2 with different shunt FACTS devices (CSC-STATCOM, VSC-STATCOM & SVC) for Case-3 (3-phase fault for 0.1s to 0.2s).

5. CONCLUSIONS

In this paper, the dynamic modeling of CSC based STATCOM is studied and pole-shifting controller for the best input-output response of CSC-STATCOM is presented, in order to enhance the transient stability of the power system with the different disturbances. The novelty in my approach lies in the fact that, transient stability of a simple two-area two-machine power system is improved and CCT of disturbances are also increased. In this work, proposed scheme is verified from MATLAB package. This paper also shows that CSC-STATCOM has more reliable and effectiveness rather than other shunt FACTS devices (SVC & VSC- STATCOM) in terms of oscillation damping, CCT and transient stability of a simple two-area power system. Finally, CSC based STATCOM can be regarded as an alternative FACTS device to that of other shunt FACTS devices (SVC & VSC-STATCOM).

REFERENCES

A. E. Hammad, “Analysis of power system stability enhancement by static Var compensators", *IEEE Trans. Power Syst.*, vol. PWRS-1, pp.222 -227, 1986.

B. Han and S. Moon "Static synchronous compensator using thyristor PWM current source inverter", *IEEE Transactions Power Delivery*, vol. 15, pp.1285, 2000.

B. T. Ooi , M. Kazerani , R. Marceau , Z. Wolanski , F. D. Galiana , D. McGillis and G. Joos "Mid-point sitting of facts devices in transmission lines", *IEEE Trans. Power Del.*, vol. 12, no. 4, pp.1717 -1722, 1997.

C. Jing, V.Vittal, G.C.Ejebe, G.D.Irissari, "Incorporation of DC and SVC Models in the Northern State Power Co (NSP) Network for on-line Implementation of Direct Transient Stability Assessment" *IEEE Trans. on Power Systems*, vol. 10, no. 2, pp. 898-906, May 1995.

C. Schauder and H. Mehta "Vector analysis and control of advanced static VAR compensators", *IEE Proceedings of Generation, Transmission and Distribution*, vol. 140, pp.299, 1993.

D. Shen and P. W. Lehn "Modeling, analysis, and control of a current source inverter-based STATCOM", *IEEE Transactions Power Delivery*, vol. 17, pp.248, 2002.

G. Sybille and P. Giroux, "Simulation of FACTS controllers using the MATLAB power system blockset and Hypersim real-time simulator", *IEEE Power Eng. Soc. Panel Session on Digital Simulations of FACTS and Custom Power Controllers, Winter Meeting*, p.p. 488-491, January 2002.

H. S. Hosseini, and A. Ajami, "Transient Stability Enhancement of AC Transmission System using STATCOM", *IEEE TENCON '02*, Vol. 3, pp.1809 - 1812, Oct. 2002.

H. Tsai, C. Chu and S. Lee, "Passivity-based Nonlinear STATCOM Controller Design for Improving Transient Stability of Power Systems", Proc. of *IEEE/PES Transmission and Distribution Conference & Exhibition*: Asia and Pacific Dalian, China, 2005.

K. T. Law , D. J. Hill and N. R. Godfrey "Robust controller structure for coordinated power system voltage regulator and stabilizer design", *IEEE Trans. Control Syst. Technol*., vol. 2, no. 3, pp.220 -232 1994.

L. Cong and Y. Wang, "Co-ordinated control of Generator excitation and STATCOM for Rotor angle stability and voltage regulation enhancement of power systems." *IEE Proceedings on Generation & Transmission and Distribution*, 149(2), pp 659-666, Feb 2002.

L. Gyugyi, "Power electronics in electric Utilities: Static VAR compensators," *Proceedings of the IEEE*, vol. 76, no. 4, pp. 483-493, Apr. 1988.

L. Gyugyi, "Application Characteristics of Converter-Based FACTS Controllers", Proceedings of *International Conference on Power System Technology (Power Con 2000)*, Piscataway, NJ, USA, vol. 1, December 2000, pp. 391-396.

M. H. Haque "Improvement of first swing stability limit by utilizing full benefit of shunt facts devices", *IEEE Trans. Power Syst*., vol. 19, no. 4, pp.1894 -1902, 2004.

M. Kazearni and Y. Ye "Comparative evaluation of three-phase PWM voltage- and current-source converter topologies in FACTS applications", *Proc. IEEE Power Eng. Soc. Summer Meeting*, vol. 1, pp.473, 2002.

N. Ali and V. Amin, "An LQR/Pole Placement Controller Design for STATCOM," *in Proc. Conf. Rec. IEEE CCC*, pp.189-193, July 2007.

N. G. Hingorani and L. Gyugyi, *Understanding FACTS: Concepts and Technology of Flexible ac Transmission Systems*, IEEE Press, New York, 1999.

Pedro Teppa-Garran, Germain Garcia, "Optimal Tuning of PI/PID/PID$^{(n-1)}$ Controllers in Active Disturbance Rejection Control", Journal of Control Engineering and Applied Informatics, Vol.15, No.4 pp. 26-36, 2013.

P. Kundur, "*Power system stability and control*." McGraw-Hill, 1994.

P. Kumkratug and M.H. Haque. "Versatile model of a unified power flow controller in a simple power system", *IEE Proc.- GTD*, Vol. 150, No. 2, pp. 155-161, 2003.

P. Rao , M. L. Crow and Z. P. Yang, "STATCOM control for power system voltage control applications", *IEEE Transactions Power Delivery*, vol. 15, no. 4, pp.1311 - 1317 2000.

Rangasamy Shivakumar, "Implementation of an Innovative Cuckoo Search Optimizer in Multi-machine Power System Stability Analysis", Journal of Control Engineering and Applied Informatics, V ol.16, No.1 pp. 98-105, 2014.

Sandeep Gupta, R. K. Tripathi, "Voltage Stability Improvement in Power Systems using FACTS Controllers: State-of-the- Art Review". *IEEE International Conference on Power, Control and Embedded Systems (ICPCES)*, pp.1-8, 2010.

Schauder, M. Gernhardt, and E. Stacey, "Operation of +/- 100MVAR TVA STATCON," *IEEE Transactions Power Delivery*, vol. 12, pp. 1805–1811, Oct. 1997.

Sidhartha Panda and Ramnarayan N. Patel,"Improving Power System Transient Stability with an Off–Centre Location of Shunt FACTS Devices," *Journal of Electrical Engineering*, vol. 57, No. 6, 365–368, 2006.

Tan, Y.L, "Analysis of line compensation by shunt-connected FACTS controllers: a comparison between SVC and STATCOM," *IEEE Power Engineering Review*, vol. 19, no.8, pp. 57-58, 1999.

Vasile Cîrtoaje, Alina Simona Baiesu, Sanda Florentina Mihalache; "Two Controller Design Procedures Using Closed-Loop Pole Placement Technique", Journal of Control Engineering and Applied Informatics, Vol.11, No. 1, pp. 34-42, 2009.

Y. L. Tan and Y. Wang "A robust nonlinear excitation and SMES controller for transient stabilization", *Int. J. Elect. Power Energy Syst.*, vol. 26, no. 5, pp.325 -332 2004.

Y. Ni, L. Jiao, S. Chen and B. Zhang, "Application of a Nonlinear PID Controller on STATCOM with a Differential Tracker," *International Conference on Energy Management and Power Delivery*, EMPD-98, New York, USA, pp. 29-34, 1998.

Y. Ye, M. Kazerani, Victor H. Quintana, "Current-Source Converter Based STATCOM: Modeling and Control", *IEEE Transactions on Power Delivery*, vol.20, no.2, April 2005.

Appendix A.

Parameters for various components used in the test system configuration of Fig. 5. (All parameters are in pu unless specified otherwise):

For generator of plant (P1 & P2):

V_G=13.8 kV; R_s= 0.003; f=50 Hz; X_d= 1.305; X_d'= 0.296; X_d''= 0.252; X_q'= 0.50; X_q''= 0.243; T_d'=1.01 s; T_d''=0.053 s; H=3.7 s

(Where R_s is stator winding resistance of generators; V_G is generator voltage (L-L), f is frequency; X_d is synchronous reactance of generators; X_d' & X_d'' are the transient and sub-transient reactance of generators in the direct-axis; X_q' & X_q'' are the transient and sub-transient reactance of generators in the quadrature-axis; T_d' & T_d'' are the transient and sub-transient open-circuit time constant; H the inertia constant of machine.)

For Excitation System of machines (M1 & M2):

Regulator gain and time constant (Ka & Ta): 200, 0.001 s; Gain and time constant of exciter (Ke & Te): 1, 0 s; Damping filter gain and time constant (Kf & Tf): 0.001, 0.1 s; Upper and lower limit of the regulator output: 0, 7.

Parameters of shunt FACTS devices:

SVC: - System nominal voltage (L-L): 500 kV; f : 50Hz; K_p=3; K_i=500; Vref = 1.

VSC-STATCOM: - System nominal voltage (L-L): 500 kV; DC link nominal voltage: 40 kV; DC link capacitance: 0.0375 μF; f: 50Hz; K_p=50; K_i=1000; Vref = 1.

CSC-STATCOM: - System nominal voltage (L-L): 500 kV; R_{dc}=0.01 Ω; L_{dc}=35 mH; C_f=400 μF;R=0.3 Ω;L = 1.8 mH; ω=314 (these parameters are used in (7)); Vref = 1.